http://journal.uir.ac.id/index.php/JGEET

E-ISSN : 2541-5794
P-ISSN : 2503-216X

Journal of Geoscience,
Engineering, Environment, and Technology
Vol 10 No 01 2025

RESEARCH ARTICLE

Quantifying hydrothermal alteration Derived by remote sensing technique in Tompaso Geothermal Field (North Sulawesi Indonesia)

Laode Bariadi, Asep Saepuloh*

Faculty of Earth Sciences and Technology, Bandung Institute of Technology, Jl. Ganesha No. 10, Bandung.

* Corresponding author : saepuloh@itb.ac.id
Tel.: +62 853-9683-3943
Received: Oct 29, 2024; Accepted: Feb 10, 2025.
DOI: 10.25299/jgeet.2025.10.1.19515

Abstract

Quantifying hydrothermal alteration is important for geothermal system modeling, which aims to understand fluid dynamics, soil distribution, and energy production potential in the geothermal exploration areas as well as the economic mineral potential at the Tompaso area, North Sulawesi. Alteration processes can result in weathering degradation of rock strength. The Sentinel-2 color composite of band ratio R,G,B for band (4/2), band (8A/11), and band (11/12) reveals the distribution of iron oxides, ferromagnesian silicates, and clay minerals. These alteration minerals are characterized by the presence of clay minerals such as chlorite (Chl), epidote (Ep), quartz (Qs), sericite (Sr), alunite (Al), and illite (ill), which formed at temperatures of 110-300^{0}C and fluid pH ranging from 3-5 (acidic in nature). The process of geological phenomena in the form of structures that open fluid pathways affects changes in the physical and chemical composition of the host rocks. The host rock and hydrothermal interactions influence to the fertility as well as vegetation conditions. Therefore, the soil and vegetation conditions were used to trace the occurrence of hydrothermal alteration minerals. A band ratio of the chlorophyll spectrum captured by the red edge vegetation index (REVI) is used as a basis for mapping vegetation stress related to the occurrence of the alteration minerals. The insitu chlorophyll measurements of ferns were used to verify the REVI in the study area. The REVI image shows anomalous vegetation stress corresponding to alteration minerals. To quantify the detection correctness, the SPAD soil measurements were conducted to pinpoint vegetation stress caused by the existence of hydrothermal alteration minerals. Correlation between alteration minerals to these two variables REVI and fern SPAD. The determination coefficient (R^2) between REVI and alteration minerals then the alteration minerals and SPAD chlorophyll measurements were archived linearly about 0.7. We have also obtained a linear correlation with positively gradient between alteration zones of argillic and propylitic presented by occurrences of kaolinite, sericite, chlorite, epidote, and quartz minerals in rock samples, to stressed vegetations.

Keywords Sentinel-2 - Tompaso - Remote sensing - Hydrothermal alteration minerals - Vegetation stress

1. Introduction

Geothermal resources presented by hydrothermal alteration are important aspect for resource exploration, which the alteration zones indicate a hot fluid pathway underlying the geothermal system. The presence of clay minerals indentified hydrothermal alteration occurrence potential (Alpine et al., 2022; Browne, 1978; Ferreiro Mählmann et al., 2024). The process of hydrothermal alteration involves the interaction of hot fluids with subsurface rocks, resulting in changes to their chemical and physical properties (Iswahyudi et al., 2014). Consequently, the quantification of hydrothermal alteration is an essential step in geology, particularly for resource estimation, geological mapping, and the mitigation of potential hazards in specific areas (Heap et al., 2020; Reyes, 1990).

We have selected West Tompaso in the Minahasa District, North Sulawesi, Indonesia, as the study area due to its high potential geothermal energy sources derived from tectonic activity along the Sangihe volcanic arc (Utami, 2011). The diversity of rock types and minerals resulting from hydrothermal alteration has significant implications for agriculture, mining, and the development of environmental mitigation strategies. The island of North Sulawesi is shaped by two active subduction zones: the Maluku Trough in the east and the Sulawesi Trough in the north (Hamilton, 1979; Simandjuntak and Barber, 1996). Regional tectonics strongly influence the geology of North Sulawesi. The North Sulawesi Arc spans the provinces of North Sulawesi and Gorontalo, extending approximately 500 km in length (from 121°E to 125°E) and 70 km in width (from 0.5°N to 2°N). The volcanic arc trends northeast-southwest and comprises several volcanoes, including Mts. Ambang, Soputan, Lokon, Mahawu, Tangkoko, Ruang, Karangetang, and Awu (Hamilton, 1979; Kusumadinata et al., 1979).

The area exhibits varying elevations, with the highest peak in the central-northern region of Sulawesi reaching 3,225 meters. Geologically, North Sulawesi is predominantly composed of limestone, which constitutes the primary formation unit of the Ratatotok Sedimentary Basin (Bellier et al., 2001; Hall, 2009; Hamilton, 1979; Silver and Moore, 1978; Sukamto and Westermann, 1992). Additionally, the region contains various other rock units, ranging from the oldest to the youngest: mudstone, Ratatotok limestone, intrusive rocks, porphyry andesite intrusions, volcanic andesite, epiclastic deposits, and alluvial deposits (Fig 1A).

Remote sensing, as defined by (Duda and Jones, 2011; Jensen, 1996; Lillesand et al., 2015), is an Earth observation technique that involves data collection without direct physical contact with the target object. This method has

proven effective in identifying geological features, including linear structures, lithology, and mineralogy. Based on the wavelength of electromagnetic radiation utilized, remote sensing can be categorized into two main types: optical and radar. Radar systems, particularly Synthetic Aperture Radar (SAR) imagery, offer the advantage of detecting linear structures by calculating contrast between geological features.

Additionally, SAR is sensitive to surface changes induced by tectonic and hydrothermal processes (Campbell and Wynne, 2011; Richards, 2009; Sabins, 1999). The interaction between electromagnetic radiation, hot fluids, and rocks in geothermal environments (Barnes, 1997; Lowell and Guilbert, 1970; Sillitoe, 2010). Facilitates the detection of mineralogical changes characteristic of hydrothermal alteration zones. For instance, quartz minerals, often dominate altered rocks and serve as indicators of intensive hydrothermal activity (Idrus et al., 2021). Similarly, feldspar minerals, as primary components of igneous rocks, can undergo transformation into secondary minerals such as kaolinite or illite through hydrothermal alteration processes (Idrus et al., 2021).

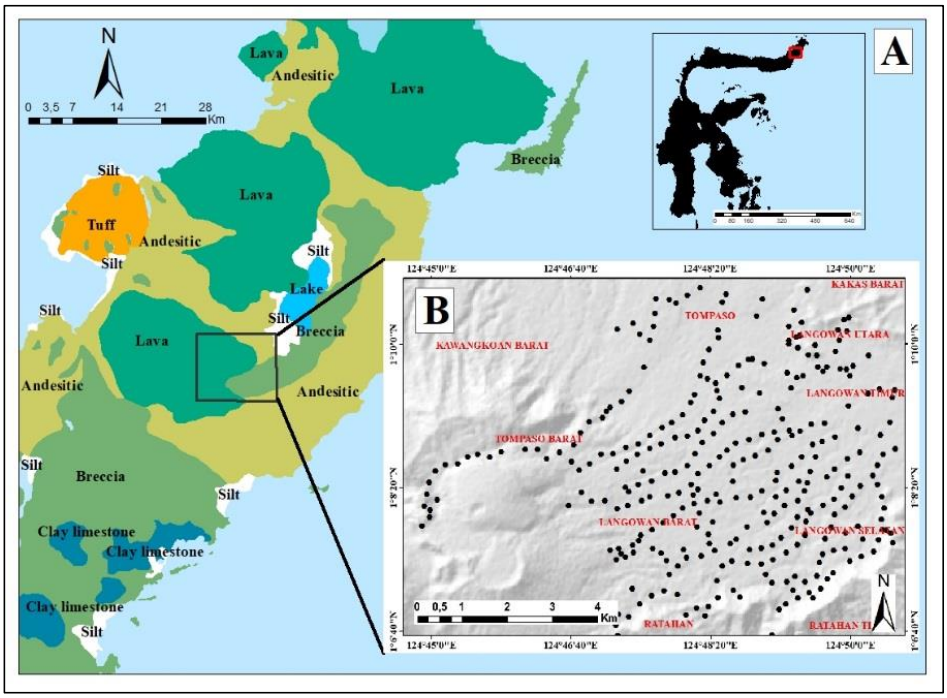

Fig 1. Regional geologic map of North Sulawesi lava, andesite, breccia, and sillt rock units (A), specifically West Tompaso subdistrict, Minahasa regency, North Sulawesi province, Indonesia (B). Black dots are the measurement locations of chlorophyll content of fern vegetation with a total of 322 SPAD points (B).

2. Methods

In this study, we analyzed the vegetation index using Sentinel-2 images, which comprise 13 spectral bands ranging from visible to shortwave infrared. The images were obtained from the European Union's Copernicus program via the data center at https://dataspace.copernicus.eu/. The Sentinel-2 image was acquired during the near-field measurement period on October 8, 2023. The specifications of the Sentinel-2 images used in this study are listed in Table 1.

Table 1. Sentinel-2 images acquired on August 9th, 2023, which has been corrected atmospherically and radiometrically used in this study. (Idrus et al., 2021).

Designated Bands	Electromagnetic Regions	Center Wavelength (nm)	Spatial Resolution (m)
B2	Visible blue (B)	490	10
B3	Visible green (G)	560	10
B4	Visible red (R)	665	10
B5	Red edge-1 (RE-1)	705	20
B6	Red edge -2 (RE-2)	740	20
B7	Red edge (RE-3)	783	20
B8A	Near-infrared narrow (NIRn)	865	20
B11	Shortwave infrared-1 (SWIR-1)	1610	20
B12	Shortwave infrared-2 (SWIR-2)	2190	20

The Sentinel-2 images underwent atmospheric correction using the Sen2Core method (Saepuloh et al., 2023). The bands utilized, with spatial resolutions ranging from 10 to 20 meters, include bands 2, 3, 4, 5, 6, 7, 8a, 11, and 12. Subsequently, a resampling method was applied to generate images with a uniform spatial resolution of 10 meters.

This study utilized a band ratio composite technique, which involves combining multiple spectral bands across various wavelengths, including near-infrared and red, to highlight specific characteristics of minerals and vegetation. The band ratios used include band ratio (4/2) for identifying green-colored clay minerals, composite band ratio (8a/11) for ferrous silicate minerals, and composite

band ratio (11/12) for detecting ferrous iron oxide minerals (Fig. 2)

We identified mineral alteration and vegetation stress occurrences using composite bands ratios and the red edge vegetation index (REVI), respectively. REVI facilitates the mapping of stressed vegetation caused by exposure to radioactive minerals and involves analyzing the distribution of volcanic rocks containing alteration minerals. This index is particularly useful for assessing the level of plant stress induced by alteration minerals by measuring chlorophyll content in plants (Saepuloh et al., 2023). The red edge vegetation index (REVI) is defined as follows:

$$\text{REVI} = \frac{(R_{B3} - R_{B4})}{(R_{B3} + R_{B4})} + \frac{(R_{B6} - R_{B4})}{(R_{B6} + R_{B4})} \quad \text{.....(1)}$$

Verification was conducted through laboratory analysis of thin sections and petrographic examination, using a total of six samples of altered rocks (Fig. 3). Reflectance measurements were performed at field sample points to assess the extent of mineral alteration. Data from photo-micrograph analysis were correlated with the red edge vegetation index values, and alteration levels were calculated based on reflectance values to determine the percentage of alteration minerals.

Verification was then conducted using photo-micrograph analysis of the rock samples to the six altered rock samples (Fig. 3). Field data from photo-micrograph analysis were correlated with REVI values, and alteration levels were quantified based on reflectance values to calculate the percentage of alteration minerals.

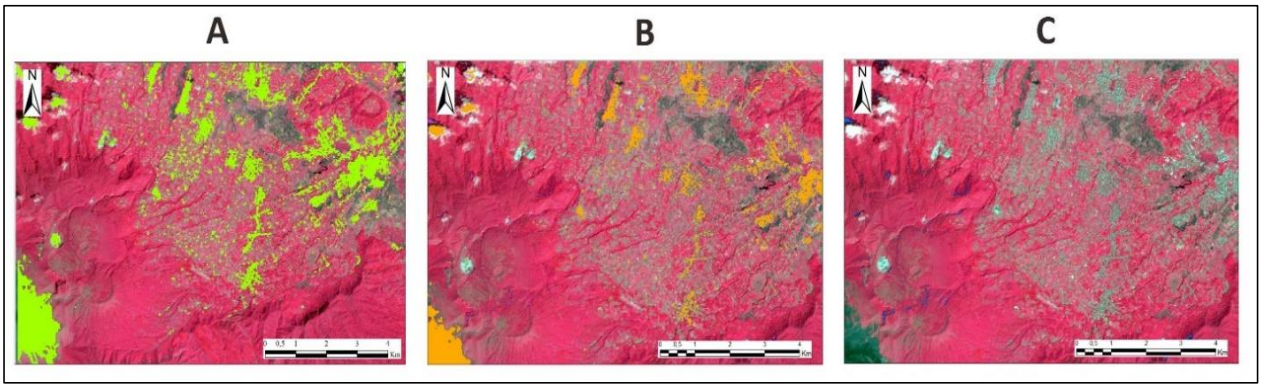

Fig 2. 2 Map depicting the distribution of alteration minerals overlaid on the R.G.B composite (B8.B4.B3) in red: clay minerals in green (A), iron silicates in orange (B), and iron oxide minerals in blue (C). based on the band ratio of Sentinel-2 images in the study area.

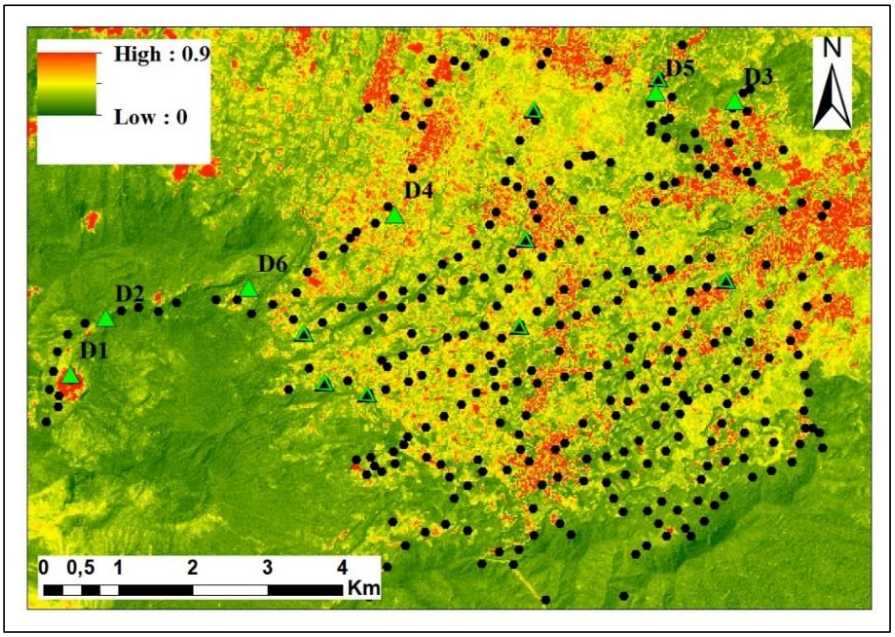

Fig 3. The red edge vegetation index (REVI) shows the high to low vegetation index indicated by the low green to high red sections overlaid with rock sampling sites (black triangles), altered rock sampling (green triangles), and SPAD chlorophyll measurements (black dots).

3. Results

3.1 Alteration Mineral Identification

Photo-micrograph thin section analysis of locations D1, D2, and D6 revealed the presence of alteration minerals, including chlorite, alunite, kaolinite, sericite, quartz, and epidote (Fig. 4). These minerals were formed at temperatures ranging from 110 to 300°C and in fluids with a pH of 3 to 5, indicating acidic conditions (Kingston Morrison, 1997). The identified minerals were associated with the argillic alteration zone, consistent with previously published findings (Corbett and Leach, 1998).

At locations D3, D4 and D5 we identified the presence of sericite, chlorite, quartz and epidote minerals (Fig. 4). These minerals were formed at low temperatures with a pH ranging from 3 to 5. The identified minerals were associated with the porphyritic alteration zone, consistent with previously published findings (Corbett and Leach, 1998).

The results of photo-micrograph analysis were correlated with remote concordance composite RGB imagery using the band ratios (8a/11), (11/12), and (4/2). The identified alteration minerals include ferrous silicates, ferrous oxides, and clay minerals (Sabins, 1999). Ferrous silicates, such as chlorite and epidote, were detected in the propylitic alteration zone, indicating an association with hydrothermal activity. Clay minerals, including kaolinite and illite, were detected in the argillic alteration zone, suggesting more advanced weathering and alteration processes. The analysis also showed that the distribution of kaolinite and illite aligns with geochemical conditions conducive to clay mineral formation (Chen et al., 2019).

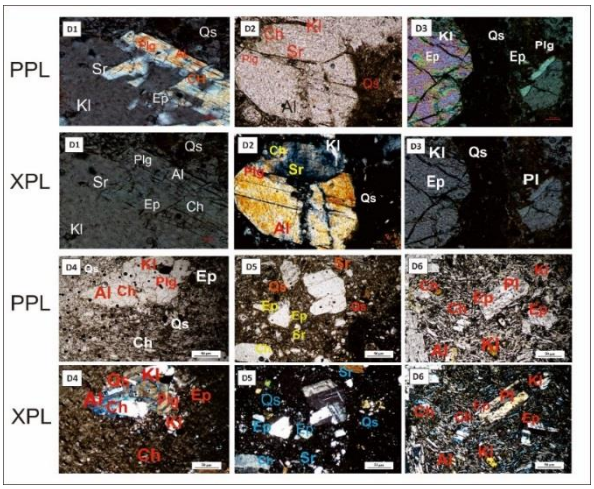

Fig 4. Visual photo-micrographs of rock samples D1, D2, D3, D4, D5 and D6 using parallel nicol (PPL) and cross nicol (XPL) for mineral identification including plagioclase (Plg), quartz (Qs), epidote (Ep), chlorite (Ch), and sericite (Sr). Notations from D1 to D6 are sample codes.

3.2. Vegetation Stress Identification

The analysis results using REVI show the classification of low and high REVI values (Fig. 3). Low REVI values indicate the presence of stressed vegetation caused by hydrothermal alteration minerals, including kaolinite, chlorite, epidote, and alunite. These minerals result from chemical and physical changes induced by hydrothermal interactions (Carranza and Hale, 2001).

A low REVI indicates reduced chlorophyll content and decreased photosynthetic activity. In contrast, healthy vegetation exhibits high REVI values, reflecting optimal photosynthetic processes (Saepuloh et al., 2023). Chlorophyll measurements using the Soil Plant Analysis Development (SPAD) method were conducted at 322 points to validate the REVI. The REVI values showed a negative linear correlation with hydrothermal alteration minerals, including kaolinite, chlorite, epidote, and alunite, indicating that hydrothermal alteration negatively impacts plant health. Furthermore, SPAD field measurements revealed that chlorophyll content in plant leaves at sites with high percentages of hydrothermal alteration was significantly lower, with SPAD values less than 25. These findings confirm that both REVI and SPAD are effective tools for identifying and monitoring vegetation stress associated with hydrothermal activities.

3.3 Correlation between alteration minerals and vegetatation stress

Ferns are a group of plants with a true vascular system, classified as Tracheophyta (Chang and Ismail*, 2019; Li et al., 2020). In the study area, these plants are evenly distributed across both lowland and highland morphological zones. Ferns are also known for their ability to adapt to highly weathered or altered environments.

Correlation analysis was conducted using linear regression to confirm the relationship between REVI and the percentage of mineral alteration observed in photo-micrographs. A strong correlation is indicated by a determination coefficient (R^2) close to +1, while a weak correlation is represented by an R^2 value close to zero (Chatterjee and Hadi, 2015).

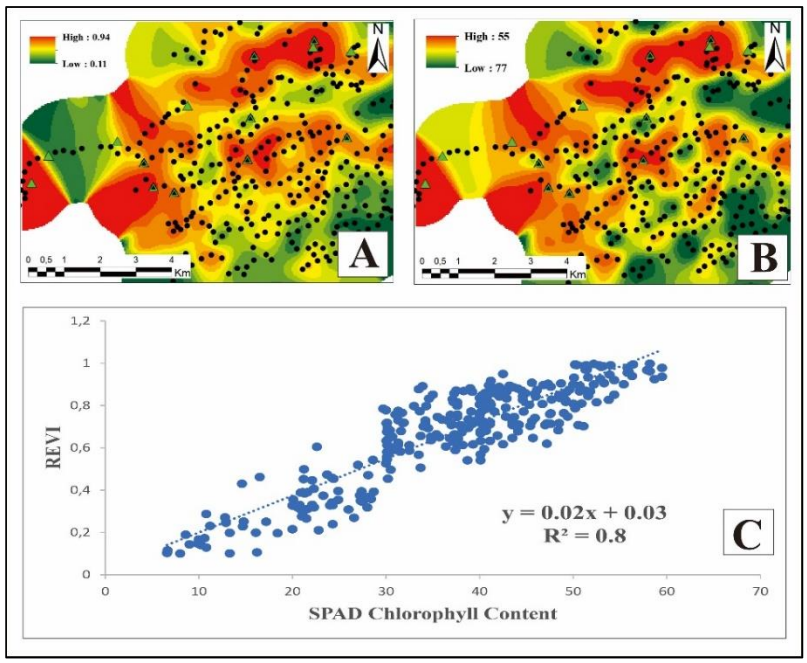

Fig 5. Kriging maps of the red edge vegetation index high to low values (A) SPAD measurement points of chlorophyll content (B) in the field (B), with their linear regression showing a coefficient the determination R^2 about 0.8.

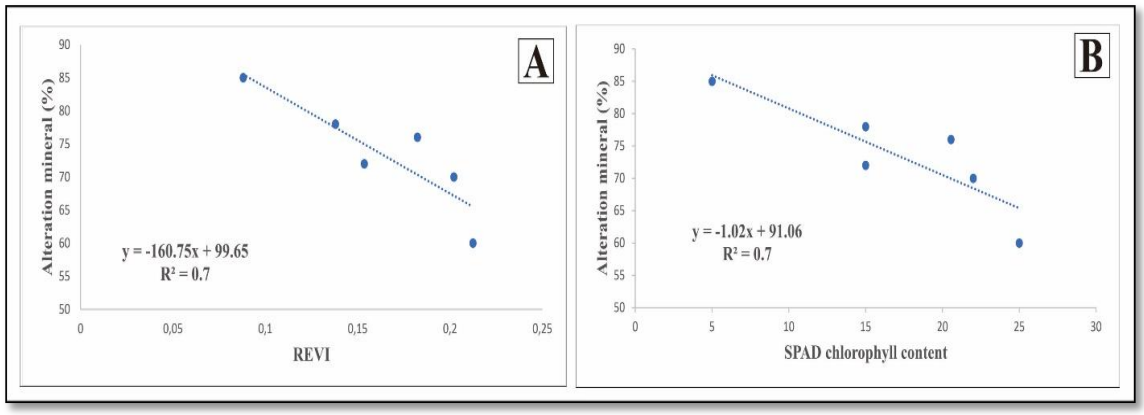

Fig 6. The correlation alteration minerals (%) with red edge vegetation index (A) and correlation of alteration minerals with chlorophyll content of ferns SPAD (B) show a coefficient of determination R^2 about 0.7.

The overall SPAD measurement data from 321 points were correlated with REVI (Fig. 5). A linear correlation was obtained, with an R^2 value of approximately 0.7 (Fig. 5C). Furthermore, the correlation between REVI and alteration minerals observed in photo-micrographs also indicates a linear relationship, with an R^2 value of approximately 0.7 (Fig. 6A).

In addition, the correlation between alteration minerals, SPAD measurement data of fern leaves, and photo-micrograph analyses indicates a linear correlation with an R^2 value of approximately 0.7 (Fig. 6B). According to the scatter plots, low REVI values (less than 1) correspond to strong vegetation stress, as indicated by SPAD values below 25. The alteration of minerals, especially those containing acidic fluids with low pH, reduces chlorophyll content. These alteration processes, particularly those involving acidic fluids, can affect vegetation health by altering the morphology of plant leaves, such as ferns, which grow in areas where hydrothermal alteration occurs (Carranza and Hale, 2001; Hede et al., 2015).

The correlation between REVI and alteration minerals shows a linear correlation, similar to the SPAD chlorophyll content (Fig. 5b). This linear relationship is associated with the vegetation stress distribution process, involving REVI composite band ratios and photo-micrograph results of altered rocks. The quantification of alteration was then performed by calculating REVI pixel values and the percentage of alteration minerals in photo-micrograph thin sections, as presented in the alteration mineral estimation map (Fig. 8).

4. Discussion

Indentifying vegetation stress based on REVI using Sentinel-2 imagery shows an index value of less than 1, which indicates stressed vegetation. The REVI is sensitive to vegetation stress, as verified by chlorophyll measurements of fern leaves with a SPAD value of less than 25. The low concordance between REVI and SPAD values corresponds to surface manifestations such as hot springs, fumaroles, and alteration zones (Fig. 7). Hydrothermal fluids alter the mineral composition of host rocks and the ground surface. According to a reported study, the ENE-SWS Soputan strike-slip fault serves as the pathway for the hydrothermal system (Lécuyer et al., 1997; Manyoe and Hutagalung, 2022; Prasetyo et al., 2015). Therefore, vegetation growing near faults experiences stress due to the interaction between soil and hydrothermal fluids (Fig. 8).

Fig 7 Plants under stress conditions (A,B,C), showing areas of surface manifestations of hot springs and fumaroles (D,E), and altered rock samples indicated by tuff alteration (F,G), and propylite alteration zones (H).

According to photo-micrograph analysis, we identified that the six altered rock samples are composed of alunite (Al) and kaolinite (Kl) minerals, which are located in argillic alteration zones, and epidote (Ep) and chlorite (Chl) minerals, which are found in porphyritic alteration zones (Table 2). These minerals provide important information about the temperature and pressure conditions during their

formation (Browne, 1978; Cumming, 2009; Mulyaningsih et al., 2021).

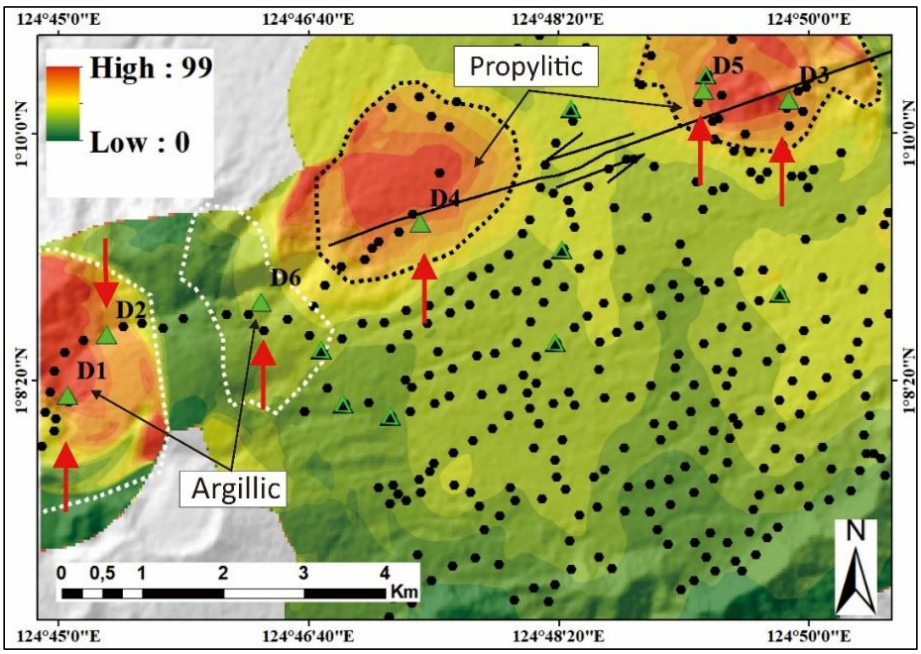

Fig 8. The kriging map of the estimated alteration zones shows a low to high alterations indicated by green to red portions overlaid on altered rocks sample presented by black triangles. The sampling locations and photo-micrograph of altered rocks are presented by red arrows and green triangles; the strike slip faults and SPAD chlorophyll measurements are presented by black lines and black dots; the white and black polygons are estimated argillic and propylitic alteration zones, respectively

Table 2. The alteration mineral percentages visual of five photo-micrograph, Chlorophyll content derived by SPAD measurement, and REVI vegetation index.

Sample ID	Primary Minerals (%)	Alteration Minerals (%)								SPAD	REVI	Alteration Type
		Chl	Al	Kl	Sr	Qs	Ep	Il	TOTAL			
D1	24	5	13	20	3	15	20	-	100	20.55	0.18	Argillic
D2	40	-	20	20	-	5	15	-	100	25	0.21	Argillic
D3	30	30	-	-	10	2.5	30	-	100	22	0.20	Propylitic
D4	22	30	-	-	30	3	15	-	100	15	0.13	Propylitic
D5	28	25	-	-	20	2	25	-	100	15	0.15	Propylitic
D6	15	10	30	30	5	-	5	5	100	5	0.08	Argillic

The correlation between REVI, chlorophyll content, and the percentage of alteration minerals shows a very strong relationship, with a determination coefficient (R^2) of about 0.7. The level of vegetation stress, indicated by low REVI, is directly proportional to the low SPAD chlorophyll value of plants in the alteration zones (Fig. 6). The stressed vegetation is located beyond the altered rocks, which contain kaolinite, epidote, chlorite, and alunite minerals (Fig. 7). The results of the calculation of the percentage of alteration minerals with REVI values show a high anomaly distribution in significant alteration zones, illustrating hydrothermal activity in the area of active fault systems (Fig. 8). These minerals were produced by hydrothermal fluids with a low pH (Heinrich, 2005). Previous studies have reported that topsoil originating from altered rocks affects plant growth due to oxidation by sulfuric acid (Carranza and Hale, 2001; Hede et al., 2015; Semenkov et al., 2021).

The use of remote sensing technology, especially Sentinel-2 imagery, in detecting the signatures of alteration minerals and alteration zones, plays an important role in the development of renewable energy sources. The ability of optical satellite imagery to detect vegetation stress and alteration minerals makes a significant contribution to understanding the environmental impacts of geothermal activities.

5. Conclusion

This study effectively quantified the hydrothermal alteration minerals in Tompaso, North Sulawesi, Indonesia, based on satellite imagery and verified through field measurements of rock samples and chlorophyll content in fern leaves.

The field measurements of chlorophyll content and the red edge vegetation index (REVI) confirmed that the stressed vegetation was located at geothermal manifestations, such as hot springs, fumaroles, and alteration zones of argillic and propylitic types.

By using field measurements of rock samples, chlorophyll content in fern leaves, and Sentinel-2 imagery, hydrothermal alteration has been effectively quantified. This study demonstrates that REVI and SPAD chlorophyll measurements successfully identified vegetation stress related to alteration, with an R^2 of about 0.7. Low REVI values (less than 1) and chlorophyll content (less than 25 SPAD) correlate with hydrothermal alteration zones, including argillic and propylitic zones, which are characterized by kaolinite, chlorite, epidote, and alunite minerals. The alteration zone distribution map illustrates the relationship between strike-slip faults and hydrothermal activity, which affect plant condition and structure.

Acknowledgments

This study was supported partially by LPPM ITB under research grant PN-6-04-2024. The thin sections were processed under Petrology and Volcanology Laboratory, Faculty of Earth Sciences and Technology, ITB. The grammar of the writing was professionally verified by sister Ririn Claudia, S.S., Gr.

References

Alpine, F., Yatini, Y., Takodama, I., 2022. Identification of Geothermal System In "Diana" Area, Indonesia Based On Magnetotelluric Data Modelling. Journal of Geoscience, Engineering, Environment, and Technology 7, 7–14.

Barnes, H.L., 1997. Geochemistry of hydrothermal ore deposits. John Wiley & Sons.

Bellier, O., Sébrier, M., Beaudouin, T., Villeneuve, M., Braucher, R., Bourles, D., Siame, L., Putranto, E., Pratomo, I., 2001. High slip rate for a low seismicity along the Palu-Koro active fault in central Sulawesi (Indonesia). Terra Nova 13, 463–470.

Browne, P., 1978. Hydrothermal alteration in active geothermal fields. Annual review of earth and planetary sciences 6, 229–248.

Campbell, J.B., Wynne, R.H., 2011. Introduction to remote sensing. Guilford press.

Carranza, E.J.M., Hale, M., 2001. Remote detection of vegetation stress for mineral exploration, in: IGARSS 2001. Scanning the Present and Resolving the Future. Proceedings. IEEE 2001 International Geoscience and Remote Sensing Symposium (Cat. No.01CH37217). pp. 1324–1326 vol.3. https://doi.org/10.1109/IGARSS.2001.976833

Chang, C.S., Ismail*, R., 2019. Biogeochemistry using Melastoma Malabathricum and fern from mineralised area in Sokor, Kelantan. IJRTE 8, 5731–5736. https://doi.org/10.35940/ijrte.D8494.118419

Chatterjee, S., Hadi, A.S., 2015. Regression analysis by example. John Wiley & Sons.

Chen, L., Yang, X., Zhen, G., 2019. Potential of Sentinel-2 data for alteration extraction in coal-bed methane reservoirs. Ore Geology Reviews 108, 134–146.

Corbett, G.J., Leach, T.M., 1998. Southwest Pacific Rim gold-copper systems: structure, alteration, and mineralization. Society of Economic Geologists Littleton, Colorado.

Cumming, W., 2009. Geothermal resource conceptual models using surface exploration data. Presented at the Proceedings, pp. 9–11.

Duda, K.A., Jones, B.K., 2011. USGS remote sensing coordination for the 2010 Haiti earthquake. Photogrammetric Engineering & Remote Sensing 77, 899–907.

Ferreiro Mählmann, R., Rahn, M., Potel, S., Nguyen-Thanh, L., Petschick, R., 2024. Determination of a normal orogenic palaeo-geothermal gradient with clay mineral and organic matter indices: a review. Swiss Journal of Geosciences 117, 17. https://doi.org/10.1186/s00015-024-00460-9

Hall, R., 2009. The Eurasian SE Asian margin as a modern example of an accretionary orogen. Geological Society, London, Special Publications 318, 351–372.

Hamilton, W.B., 1979. Tectonics of the Indonesian region. US Government Printing Office.

Heap, M.J., Gravley, D.M., Kennedy, B.M., Gilg, H.A., Bertolett, E., Barker, S.L.L., 2020. Quantifying the role of hydrothermal alteration in creating geothermal and epithermal mineral resources: The Ohakuri ignimbrite (Taupō Volcanic Zone, New Zealand). Journal of Volcanology and Geothermal Research 390, 106703. https://doi.org/10.1016/j.jvolgeores.2019.106703

Hede, A.N.H., Kashiwaya, K., Koike, K., Sakurai, S., 2015. A new vegetation index for detecting vegetation anomalies due to mineral deposits with application to a tropical forest area. Remote Sensing of Environment 171, 83–97. https://doi.org/10.1016/j.rse.2015.10.006

Heinrich, C.A., 2005. The physical and chemical evolution of low-salinity magmatic fluids at the porphyry to epithermal transition: a thermodynamic study. Miner Deposita 39, 864–889. https://doi.org/10.1007/s00126-004-0461-9

Idrus, A., Ubaidillah, A.S., Warmada, I.W., Maula, S., 2021. Geology, Rock Geochemistry and Ore Fluid Characteristics of the Brambang Copper-Gold Porphyry Prospect, Lombok Island, Indonesia. Journal of Geoscience, Engineering, Environment, and Technology 6, 67–73.

Iswahyudi, S., Saepuloh, A., Widagdo, A., 2014. Delineating Outflow Zones Using Linear Features Density (Lfd) Derived From Landsat Imagery At Paguyangan, Brebes, Central Java.

Jensen, J.R., 1996. Introductory digital image processing: a remote sensing perspective.

Kingston Morrison, 1997. Important hydrothermal minerals and their significance, 7th ed. Geothermal and Mineral Service Devision.

Kusumadinata, K., Hadian, R., Hamidi, S., Reksowirogo, L., 1979. Data dasar gunungapi Indonesia. Direktorat Vulkanologi, Bandung 820.

Lécuyer, F., Bellier, O., Gourgaud, A., Vincent, P.M., 1997. Tectonique active du Nord-Est de Sulawesi (Indonésie) et contrôle structural de la caldeira de Tondano. Comptes Rendus de l'Académie des Sciences-Series IIA-Earth and Planetary Science 325, 607–613.

Li, L., Wu, J., Lu, J., Xu, J., 2020. Speciation, risks and isotope-based source apportionment of trace elements in soils of the northeastern Qinghai–Tibet Plateau. Geochemistry: Exploration, Environment, Analysis 20, 315–322. https://doi.org/10.1144/geochem2019-042

Lillesand, T., Kiefer, R.W., Chipman, J., 2015. Remote sensing and image interpretation. John Wiley & Sons.

Lowell, J.D., Guilbert, J.M., 1970. Lateral and vertical alteration-mineralization zoning in porphyry ore deposits. Economic geology 65, 373–408.

Manyoe, I.N., Hutagalung, R., 2022. Application of lineament density extraction based on digital elevation model for geological structures control analysis in Suwawa Geothermal Area. Journal of Geoscience, Engineering, Environment, and Technology 7, 117–123.

Mulyaningsih, S., Sukisman, Y.R.S., Hidayah, R.A., 2021. Hydrothermal Alteration and Ore Metal Mineralisation at Temon, Pacitan, East Jawa,

Indonesia. Journal of Geoscience, Engineering, Environment, and Technology 6, 24–33.
Prasetyo, I., Sardiyanto, K.H., Thamrin, M.H., 2015. Clay alteration study from wells of Tompaso Geothermal Field, north Sulawesi, Indonesia, in: Proceedings World Geothermal Congress.
Reyes, A.G., 1990. Petrology of Philippine geothermal systems and the application of alteration mineralogy to their assessment. Journal of Volcanology and Geothermal Research 43, 279–309. https://doi.org/10.1016/0377-0273(90)90057-M
Richards, J.A., 2009. Remote sensing with imaging radar. Springer.
Sabins, F.F., 1999. Remote sensing for mineral exploration. Ore Geology Reviews 14, 157–183. https://doi.org/10.1016/S0169-1368(99)00007-4
Saepuloh, A., Ratnanta, I., Hede, A., Susanto, V., Sucipta, I.G.B., 2023. Radioactive remote signatures derived from Sentinel-2 images and field verification in West Sulawesi, Indonesia. Environmental Monitoring and Assessment 195. https://doi.org/10.1007/s10661-023-11868-5
Semenkov, I.N., Klink, G.V., Lebedeva, M.P., Krupskaya, V.V., Chernov, M.S., Dorzhieva, O.V., Kazinskiy, M.T., Sokolov, V.N., Zavadskaya, A.V., 2021. The variability of soils and vegetation of hydrothermal fields in the Valley of Geysers at Kamchatka Peninsula. Scientific Reports 11, 11077. https://doi.org/10.1038/s41598-021-90712-7
Sillitoe, R.H., 2010. Porphyry copper systems. Economic geology 105, 3–41.
Silver, E.A., Moore, J.C., 1978. The Molucca sea collision zone, Indonesia. Journal of Geophysical Research: Solid Earth 83, 1681–1691.
Simandjuntak, T.O., Barber, A.J., 1996. Contrasting tectonic styles in the Neogene orogenic belts of Indonesia. Geological Society, London, Special Publications 106, 185–201.
Sukamto, R., Westermann, G., 1992. Indonesia and Papua new guinea, in: The Jurassic of the Circum-Pacific. Cambridge University Press USA, pp. 183–193.
Utami, P., 2011. Hydrothermal alteration and the evolution of the Lahendong geothermal system, North Sulawesi, Indonesia.